

A Low-Communication Distributed State-Estimation Framework for Satellite Formations

Rafael Cordeiro
Instituto Superior Técnico
Universidade de Lisboa
Lisbon, PT 1049-001
rafael.andre.alves@tecnico.ulisboa.pt

Rodrigo Ventura
ISR - Instituto Superior Técnico
Universidade de Lisboa
Lisbon, PT 1049-001
rodrigo.ventura@isr.tecnico.ulisboa.pt

João Gomes
ISR - Instituto Superior Técnico
Universidade de Lisboa
Lisbon, PT 1049-001
jpg@isr.tecnico.ulisboa.pt

Zachary Manchester
Robotics Institute
Carnegie Mellon University
Pittsburgh, PA 15213
zacm@cmu.edu

Abstract— This paper presents a novel distributed state-estimation framework for satellite formations. Existing consensus-based distributed filters have high communication requirements that make them unsuitable for resource-constrained small-spacecraft formations. We present a low-communication distributed filtering scheme targeted at small-satellite formations that are limited by inter-satellite communication channel capacity. We assume a chief-deputy topology, similar to the proposed NASA *Helioswarm* mission. Our novel state-estimation framework is based on decoupling the chief state estimation filter from the deputies and using two separate filter architectures: one chief-specific that accounts for intermittent access to inertial position measurements, and a second deputy-specific one that only incorporates relative range measurements between the spacecraft, having the chief state as an external model input. We introduce a consider-covariance technique to account for the chief’s state uncertainty in the deputy’s filter. We demonstrate that the proposed distributed filter architecture requires significantly less communication than prior consensus-based methods in the literature while achieving comparable accuracy.

including more efficient scalability and greater robustness to individual failures [3], [4].

A prominent area of research in multi-agent systems within the aerospace community in recent years has been distributed localization of spacecraft formations or swarms. As the trend toward reducing the overall size, mass, and cost of individual spacecraft continues [5], [6], combining larger numbers of smaller spacecraft into formations to achieve complex missions with lower overall costs has become increasingly attractive [7], [8]. Often, such formations have a hub spacecraft, referred to as the *chief*, with more robust power, sensing, and communication capabilities, and multiple smaller *deputy* spacecraft. This is the case in several upcoming missions, such as the National Aeronautics and Space Administration (NASA) *Helioswarm* mission [9] and other international missions from European Space Agency (ESA) and the Canadian Space Agency (CSA) [10], [11], [12]. For many of these missions, even though the computational capabilities of small satellites may be limited, the limits on inter-satellite communications are often more severe.

TABLE OF CONTENTS

1. INTRODUCTION	1
2. PRELIMINARIES	2
3. PROBLEM FORMULATION	4
4. DEPUTY-CHIEF CORRELATION VIA CONSIDER COVARIANCE	5
5. EVENT-TRIGGERED UPDATES	5
6. PROPOSED LOW-COMMUNICATION DISTRIBUTED STATE-ESTIMATION FRAMEWORK ..	6
7. SIMULATION EXPERIMENTS	6
8. CONCLUSIONS	10
ACKNOWLEDGMENTS	10
REFERENCES	10
BIOGRAPHY	12

1. INTRODUCTION

Multi-agent systems have attracted great attention across fields such as physics, robotics, and aerospace engineering in recent years [1], [2]. The ability to allow multiple entities, using only local processing, to collaborate toward achieving the same global objective can result in numerous benefits,

Only a few efforts applying distributed state-estimation techniques to multi-spacecraft systems exist in the literature: Wang [13] developed a consensus-based Extended Kalman Filter (EKF) for a network of spacecraft with both relative range-only and angle-only measurements that referenced the problem of limited communication resources, and developed a sub-optimal consensus-based EKF that relies on approximations of the covariance update rules, initially introduced by Olfati-Saber [14]. Dumitriu [15] proposed a distributed navigation system based on covariance intersection, while Battistelli [16] suggested that these procedures can be reduced to the consensus-based procedures with a single consensus step for Gaussian PDFs. However, the multistep consensus algorithm [17] relies on continuous communications between agents through multiple consensus rounds, where large amounts of data, generally corresponding to information pairs, are passed concurrently. This places a heavy burden on the communication network, both in relation to the amount of data sent between agents, and also in terms of the number and frequency of communication events.

This paper tackles the distributed multi-agent localization problem for small-spacecraft formations. Such formations have limited computational and communication capabilities, making previously developed consensus-based distributed filters ill-suited. We propose a novel low-communication approach to distributed state estimation, specific for small-satellite formations with both restrictions on computational

performance and communication capacity. Our solution is based on decoupling the estimator according to the standard Chief/Deputy formation setting into two separate filters with sensor-selection utility functions based on the Crámer-Rao Lower Bound (CRLB) [18], [19] to minimize communication. This new filter architecture for each agent accounts for cross-correlations using a *consider covariance* strategy that allows one to assess the impact of neglecting unknown or possibly poorly modeled parameters on the accuracy of the state estimate. Finally, we intend to evaluate the proposed state-estimation framework on a future mission where the code will be flight-tested. Our contributions include:

- A novel low-communication state estimation framework targeted for small-satellite formations with limited computational power and communication capacity
- A set of event-triggered conditions that perform sensor selection based on the CRLB to minimize communications while achieving a desired level of accuracy
- Comparisons of accuracy and communication efficiency of the proposed low-communication framework against state-of-the-art consensus-based distributed estimators for small-satellite formations.

The paper proceeds as follows: We first introduce notation, detail the dynamics and measurement models used for each spacecraft and introduce introductory concepts to event-triggering in section 2. Next, the problem formulation regarding low-communication distributed frameworks is discussed in section 3, followed by the development of our proposed *consider covariance* solution in section 4 and the extension of the proposed algorithm with event triggering procedures in sections 5 and 6. Finally, we present simulation experiments in section 7 to validate our proposed algorithm, followed by a summary of our conclusions and future work in section 8.

2. PRELIMINARIES

Non-linear State Estimation

The filtering problem in the presence of non-linearities in the dynamics and measurement models is commonly solved with the implementation of an Extended Kalman Filter [20].

Firstly, with no loss of generality, a system with no external inputs will be considered for the purposes of a simpler algorithm deduction, where the non-linear dynamics

$$x_{k+1} = f_k(x_k) + w_k \quad (1)$$

$$y_k = h_k(x_k) + v_k \quad (2)$$

have two components of independent, zero-mean white Gaussian noise and covariance matrix described by

$$E[v_k v_k^T] = R_k \quad E[w_k e_k^T] = Q_k \quad (3)$$

and x_0 being the system initial condition that is considered to be a Gaussian random vector, $x_0 = \mathbb{N}(\bar{x}_0, \Sigma_0)$.

Assuming $Y_1^k = \{y_1, \dots, y_k\}$ to be a set of system measurements, the goal of the filter is to obtain a refined estimate of the system's state based on fusing these measurements with the dynamic propagation of the state vector.

Contrary to the normal Kalman Filter (KF) that evaluates the

condition mean of the *pdf* of x_k given Y_1^k , with non-linear dynamics, these conditional probability density functions are no longer Gaussian, which represents a heavy computational burden to propagate the entire *pdf*. The EKF, as a solution to this problem, provides an approximation of the optimal estimate, where the non-linearities of the system's dynamics are approximated by a linearized version around the last state estimate, as seen in algorithm 1.

Algorithm 1: Extended Kalman Filter

1. Prediction:

$$\hat{x}_{k+1|k} = f(x_k, w_k); \\ P_{k+1|k} = F_k P_k F_k^T + Q_k;$$

2. Update:

$$K_{k+1} = P_{k+1|k} H_{k+1}^T \cdot [H_{k+1} P_{k+1|k} H_{k+1}^T + R_{k+1}]^{-1}; \\ P_k = (I - K_{k+1} H_{k+1}) \cdot P_{k+1|k}; \\ \hat{x}_{k+1} = \hat{x}_{k+1|k} + K_{k+1} \cdot [z - h(x_{k+1|k}, v_{k+1})];$$

In algorithm 1, $P_{k+1|k}$ and P_k corresponds to the *a priori* and *a posteriori* covariance matrices [21], respectively, while $F_k = \partial f / \partial x$ and $H_k = \partial h / \partial x$ correspond to the dynamics and measurement model jacobians, respectively.

Distributed Consensus-Based Extended Kalman Filter

An initial distributed framework can be implemented using a consensus filter [17][13]. The distributed consensus-based framework is based on each spacecraft having its individual model and recursively communicating with its neighbours to reach a consensus average on a given state. This allows each satellite to improve the overall accuracy of their filter with the information from the agents in the formation.

In terms of the distributed architecture, The communication will be determined based only on an undirected communication graph network described by $G = (\mathbb{N}, \mathbb{A})$, where $\mathbb{N} = [1, \dots, N]$ is the set of spacecraft in the formation and \mathbb{A} is the set of edges, such that if (i, j) is in \mathbb{A} , there is a communication link between the i -th and the j -th spacecraft.

At each iteration, the first procedure is the local consensus state estimate. As explained previously, this corresponds to the information matrix and vector of the state. Thus at instant k , each spacecraft $j \in \mathbb{N}$ from the novel measurement set $y_k^{(i)}$, determines

- The Novel Information Pair $(\delta\Omega_{k|k-1}^{(i)}, \delta q_{k|k-1}^{(i)})$, where $\delta\Omega_{k|k-1}^{(i)} = (H_k^{(i)})^T V_k^{(i)} H_k^{(i)}$ and $\delta q_{k|k-1}^{(i)} = (H_k^{(i)})^T V_k^{(i)} y_k^{(i)}$. The term $V_k^{(i)}$ is a positive definite matrix, where the commonly used choice corresponds to the estimate of the inverse covariance of the process disturbance regarding the measurement noise v_k .

After each satellite determines its information pair from the novel measurements, the next step corresponds to finding the formation consensus state estimate by performing a consensus algorithm iterated L times and performing at each time a regional average of this pair from the communications between neighboring satellites. The consensus rounds can be seen in eq. (4), they include a set of consensus weights that correspond to the importance given to the information of each satellite.

$$\delta\Omega_k^{(i)}(l+1) = \sum_{j \in \mathbb{N}_\square} \pi^{ij} \delta\Omega_k^{(j)}(l) \quad (4)$$

$$\delta q_k^{(i)}(l+1) = \sum_{j \in \mathbb{N}_\square} \pi^{ij} \delta q_k^{(j)}(l) \quad (5)$$

In the end, the state estimate is refined with the correction of the information pair (information matrix $\Omega_k^{(i)}$ and vector $q_k^{(i)}$) that results from the consensus rounds. After this, the next iteration state is estimated through the propagation of the dynamic equations, followed by a new estimate of the information vector and matrix for the next iteration, as seen in algorithm 2.

Algorithm 2: Distributed Consensus-based Extended Kalman Filter

Initialisation: a priori values

for $g \in \mathbb{N}$ **do**

1. Compute the local correction terms

$$\delta q_k^{(g)}, \delta\Omega_k^{(g)}:$$

$$H_k^{(g)} = \frac{\partial h^g}{\partial x}(x_k|k-1)$$

$$\bar{y}_k^{(g)} = y_k^{(g)} - h^g(x_k|k-1) + H_k^{(g)} x_k|k-1$$

$$\delta\Omega_k^{(g)} = (H_k^{(g)})^T V_k^{(g)} H_k^{(g)}$$

$$\delta q_k^{(g)} = (H_k^{(g)})^T V_k^{(g)} \bar{y}_k^{(g)}$$

2. Consensus Rounds:

$$\delta q_k^{(i)}(0) \leftarrow \delta q_k^{(i)}$$

$$\delta\Omega_k^{(i)}(0) \leftarrow \delta\Omega_k^{(i)}$$

for $l = 0, \dots, L$ **do**

$$\delta\Omega_k^{(i)}(l+1) = \sum_{j \in \mathbb{N}_\square} \pi^{ij} \delta\Omega_k^{(j)}(l)$$

$$\delta q_k^{(i)}(l+1) = \sum_{j \in \mathbb{N}_\square} \pi^{ij} \delta q_k^{(j)}(l)$$

3. Perform the Estimation for each Sat.:

for $i \in \mathbb{N}$ **do**

4. Consensus Correction:

$$q_{k|k}^{(i)} = q_{k|k-1}^{(i)} + \gamma_k^{(i)} \delta q_k^{(i)}(L)$$

$$\Omega_{k|k}^{(i)} = \Omega_{k|k-1}^{(i)} + \gamma_k^{(i)} \delta\Omega_k^{(i)}(L)$$

$$\hat{x}_{k|k}^{(i)} = (\Omega_{k|k}^{(i)})^{-1} q_{k|k}^{(i)}$$

5. Prediction Step:

$$\hat{x}_{k+1|k}^{(i)} = f(\hat{x}_{k|k}^{(i)}), \text{ and } F_k^{(i)} = \frac{\delta f}{\delta x} \hat{x}_{k|k}^{(i)}$$

$$\Omega_{k+1|k}^{(i)} =$$

$$W - W F_k^{(i)} (\Omega_{k|k}^{(i)} + (F_k^{(i)})^T W F_k^{(i)})^{-1} (F_k^{(i)})^T W$$

$$q_{k+1|k}^{(i)} = \Omega_{k+1|k}^{(i)} \hat{x}_{k+1|k}^{(i)}$$

Consider Extended Kalman Filter

Consider covariance [22] analysis is a technique to assess the impact of neglecting these unknown or possibly poorly modeled parameters on the accuracy of the state estimate, thus providing a realistic estimate of the achievable accuracy of the system without the extra computational requirements of considering these parameters in the state model.

By applying the *consider covariance* technique to the previously mentioned EKF along with *a priori* information on specific consider parameters, \mathbf{c} , it is possible to improve the filter divergence characteristics due to a more accurate representation of the errors in the dynamic and measurement models.

In order to formulate the architecture of this procedure, the first step corresponds to understanding the new dynamic and measurement model functions that now have the consider parameters as an input variable,

$$\begin{cases} x_{k+1} = f(x_k, \mathbf{c}) + \mathbf{w}_k \\ y_k = h(x_k, \mathbf{c}) + \mathbf{v}_k \end{cases} \quad (6)$$

as a result the new covariance can be modeled by

$$P_{ck} = E[(\tilde{x})(\tilde{x})^T] \quad (7)$$

where

$$\tilde{x} = F_{xx}(\hat{x}_k - x_k) + F_{xc}(\bar{\mathbf{c}} - \mathbf{c}) \quad (8)$$

which leads to

$$\begin{aligned} P_c &= E[(F_{xx}(\hat{x}_k - x_k) + F_{xc}(\bar{\mathbf{c}} - \mathbf{c}))(\mathbf{F}_{xx}(\hat{x}_k - x_k) + \mathbf{F}_{xc}(\bar{\mathbf{c}} - \mathbf{c}))^T] \\ &= F_{xx} P_a F_{xx}^T + F_{xx} P_{xc} F_{xc}^T \\ &\quad + F_{xc} P_{xc} F_{xx}^T + F_{xc} P_{cc} F_{xc}' \end{aligned} \quad (9)$$

Where F_{xc} corresponds to the jacobians of the state dynamics model with respect to the consider parameters. There are two new covariance matrices, P_{xc} and P_{cc} that correspond to the correlations between state and consider parameters in addition to their associated covariance estimate, respectively. As a consequence, in this design tool, it is assumed that the consider parameters are constant throughout one iteration and that their *a priori* estimated and associated covariance matrix is known.

Spacecraft Dynamics Model

Throughout this work, we consider a set of N spacecraft in Low Earth Orbit (LEO) with positions r_i , velocities v_i , and state vectors $x_i = [r_i; v_i]$ expressed in the Earth Centered Inertial (ECI) reference frame [23].

The dynamics model used for simulation accounts for the gravitational acceleration of the Earth up to and including the J2 term, as well as atmospheric drag. The dynamic equations can be expressed in continuous time as,

$$\dot{r}_i = v_i, \quad (10)$$

and

$$\dot{v}_i = g_i + d_i, \quad (11)$$

where g_i includes gravitational terms up to J2 and d_i corresponds to the drag.

This leads to the continuous state x , that is governed by

$$\dot{x} = g(t, x). \quad (12)$$

We use the classic 4th Order Runge-Kutta (RK4) method to discretize (12) in time, and also add zero-mean white Gaussian process noise w_k to account for uncertainty in the drag force and additional unmodeled dynamics terms, resulting in

$$x_{k+1} = f(t_k, x_k) + w_k. \quad (13)$$

Spacecraft Measurement Model

Our measurement model is inspired by the *V-R3x* mission [24], and includes a set of deputy spacecraft that are able to measure their range to other spacecraft in the formation through radio time-of-flight measurements, and a chief satellite with GNSS capabilities. This arrangement is also common of many other small-satellite missions [9], [12].

We model relative-range measurements between spacecraft i and j as

$$y_{ij} = \|r_j - r_i\|_2 + v_k \quad (14)$$

where v_k corresponds to a zero-mean white Gaussian measurement noise.

The measurement schedule selected corresponds to a sampling period of 60 seconds.

Crámer-Rao Lower Bound

The CRLB states that the covariance of any unbiased estimator is at least as high as the inverse of the Fisher information,

$$P \geq P^* \triangleq J^{-1}. \quad (15)$$

In order to reach a computation procedure for unbiased estimators for nonlinear systems in which the state variables can be assumed to be deterministic, such as the EKF, Taylor [18] proves that the inverse Fisher information matrix (P^*) corresponding to a dynamic system modeled by a nonlinear time-varying state vector differential equation with deterministic inputs and non-linear time-varying observations of the state variables corrupted by additive Gaussian white noise sequences propagates according to the same equations as the filter covariance matrix for an EKF linearized about the (unknown) true trajectory. This result allows the computation of the CRLB for this class of problems with low computational effort by propagating the Fisher information matrix:

$$J_k = (F_{k-1}^{-1})^T J_{k-1} (F_{k-1}^{-1}) + H_k^T R_k^{-1} H_k. \quad (16)$$

3. PROBLEM FORMULATION

The main objective of the present work is to estimate the state of a spacecraft formation while minimizing communication. We assume that only a single chief spacecraft has access to GPS measurements, while all other deputy spacecraft have access to relative-range measurements. We decouple the state-estimation problem into two separate filter algorithms: one chief-specific filter that includes only GPS measurements and estimates only the chief state; and a second deputy-specific one that includes relative-range measurements, treats the chief state as a parameter (not part of the filter state), and

estimates the deputy states. This architecture is illustrated in fig. 1.

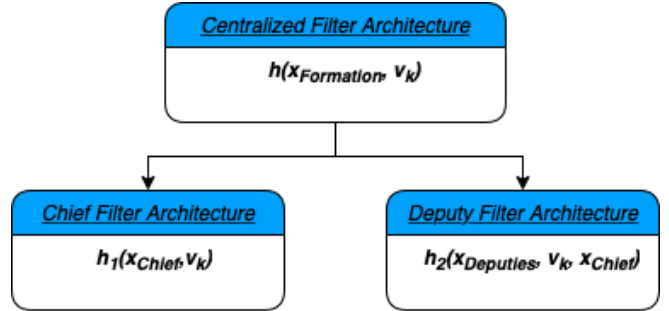


Figure 1. Decoupling scheme in terms of the measurement model inputs.

The primary difference between the centralized filter and the proposed decoupled filter architecture is that cross-covariance terms between the chief state and the deputy states are ignored. Essentially, the deputies assume that the chief's state is perfectly known. This approximation is justified if the GPS measurements available to the chief are much more accurate than the relative-range measurements available to the deputies, but will always lead to optimistic estimates that underestimate the true uncertainty.

Following the standard notation in the distributed-systems literature [25], [26], the entire formation can be described by an undirected communication graph network described by $G = (\mathbb{N}, \mathbb{A})$ where $\mathbb{N} \triangleq \{i : (i,j) \in \mathbb{A}\}$ is the set of nodes in the graph structure and \mathbb{A} is the set of arcs (connections) between nodes in the formation. A node in this structure can be regarded as a spacecraft in the formation, however, this graph structure can now be divided into communication nodes that only have processing and communications capabilities \mathbb{C} , and measurement nodes \mathbb{D} that also have sensing capabilities, thus the network can now be denoted by the triplet $G = (\mathbb{C}, \mathbb{D}, \mathbb{A})$, where $\mathbb{N} = \mathbb{C} \cup \mathbb{D}$. The proposed segmentation, comes from the further necessity of having a logical division between spacecraft that have sensing capabilities in a given instant and those who can only communicate their estimate.

The proposed decoupled filtering architecture divides the fully centralized filter into a chief-specific filter, where the measurement model only includes the chief's GPS measurements, and a deputy-specific filter that only includes relative-range measurements to neighboring spacecraft. As a result, the formation will be divided into the chief, which will be regarded as a communication node, and deputies, which will be regarded as measurement nodes. This logical separation comes from the deputies exchanging local measurements with other spacecraft while the chief only exchanges its estimates, as seen in fig. 2.

The state of each filter can be described by $x_i = [r_i, v_i] \forall i \in \mathbb{C}$ for each chief filter and $x_j = [r_1, v_1, \dots, r_n, v_n] \forall n \in \mathbb{D}$ for each deputy spacecraft. The corresponding system model for the chiefs will be

$$\begin{cases} x_{k+1}^i = f(x_k^i, t_k) + w_k^i \\ y_k^i = h(x_k^i) + v_k^i \end{cases}, \quad \forall i \in \mathbb{C} \quad (17)$$

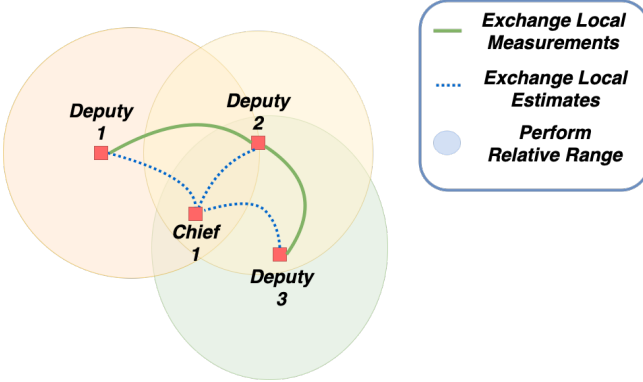


Figure 2. Representation of a four satellite graph network in terms of communication and measurement nodes.

and the corresponding system model for the deputies will be

$$\begin{cases} x_{k+1}^j = f(x_k^j, t_k) + w_k^j \\ y_k^j = h(x_k^j, x_k^i) + v_k^j \end{cases}, \quad \forall j \in \mathbb{D} \text{ and } \forall i \in \mathbb{C} \quad (18)$$

We note that, since the range measurements are symmetric (i.e. $y_k^j = y_k^i$), the total number of range measurements is $D(D + 1)/2$ where D is the number of deputies.

The biggest downside of this decoupling scheme is that the deputy filter does not take into account the uncertainty in the chief state. Therefore, the estimated covariance matrix tends to underestimate the true covariance matrix, which can lead to statistical inconsistency.

4. DEPUTY-CHIEF CORRELATION VIA CONSIDER COVARIANCE

In order to account for the correlation between chief and deputies and avoid having an inconsistent filter, we utilize the concept of *consider covariance* [27], which accounts for uncertainty in problem parameters — referred to as *consider parameters* — not included in the filter state vector. If we were to augment the deputy filter state with the chief state, $x_{aug} = [x_{Deputies}; x_{Chief}]$, the covariance matrix and the process noise covariance would have the following form,

$$P_a = \begin{bmatrix} P_{DD} & P_{DC} \\ P_{DC}^T & P_{CC} \end{bmatrix} \quad Q_a = \begin{bmatrix} Q & 0 \\ 0 & 0 \end{bmatrix} \quad (19)$$

where P_{DC}, P_{CC} include the correlations between chief and deputies in addition to the chief covariance matrix. It is also important to note that in Q_a , the zero blocks are a direct result of the process noise of the deputies not influencing the chief position. This extends to P_{CC} , as the chief dynamics does not influence the deputies orbital equations.

The dynamics and measurement Jacobians can be expressed as

$$F_a = \begin{bmatrix} F & F_c \\ 0 & I \end{bmatrix} \quad H_a = [H \quad H_c] \quad (20)$$

The inclusion of the chief estimate influence on the model leads to a new covariance propagation that follows a similar

expansion for both dynamics and measurement model. The new covariance can be modeled, with x being the state and c the added consider parameter, by the previous eqs. (7) to (9).

For the present case, F_c will be zero since the chief position does not influence the deputy position propagation, while in the case of the measurement model, the chief uncertainty will directly influence the model output, more specifically in the correction stage of the EKF, as the consider parameters do not update in the deputy filter, the new augmented filter gain matrix is

$$K_a = \begin{bmatrix} K_x \\ 0 \end{bmatrix}. \quad (21)$$

Following the same line of thinking for eq. (9),

$$\begin{aligned} K_x = & [P_a H_{k+1}^T + P_{xc} H_c^T] \\ & \cdot [H_{k+1} P_a H_{k+1}^T + R_{k+1} + H_{k+1} P_{xc} H_c^T \\ & + H_c P_{xc} H_{k+1}^T + H_c P_{cc} H_c^T]^{-1}. \end{aligned} \quad (22)$$

Inserting these expressions into the Joseph form of the Kalman filter covariance update results in,

$$P_a^+ = (I - K_a H_a) P_a^- (I - K_a H_a)^T + K_a R K_a^T, \quad (23)$$

which can be simplified to

$$P_a = (I - K_x H_{k+1}) \cdot P_a - K_x H_c P_{xc}^T \quad (24)$$

This new approach applies the *consider covariance* scheme to the decoupled EKF architecture, where now both the *a priori* estimate and associated covariance matrix are retrieved from deputy-chief communications, and the uncertainty in the chief state is handled as a consider parameter in the deputy filter. This allows the deputy filters to reason about uncertainty in the chief state to maintain statistical consistency.

5. EVENT-TRIGGERED UPDATES

To minimize communication events between spacecraft, we propose an event-triggered scheme that only performs measurement updates when a certain error threshold is exceeded. We base our error condition on the CRLB, which provides a theoretical lower bound on the covariance and can be achieved by an estimator like the EKF [18].

The current literature proved that the most prominent procedures for sensor selection rely on formulating a convex relaxation on the minimization of the *trace* of the covariance matrix [28], [29] or directly the CRLB [19].

We propose update conditions for both the chief and deputy filters based on comparing the current filter covariance to the CRLB: If the trace of the filter covariance exceeds the trace of the CRLB beyond some tolerance, a measurement update is performed:

$$\beta^c = \text{tr}(P_k^{(i)}) > \delta^c \cdot \text{tr}((P_k^*)^{(i)}), \quad \forall i \in \mathbb{C} \quad (25)$$

$$\beta^d = \text{tr}(P_k^{(j)}) > \delta^d \cdot \text{tr}((P_k^*)^{(j)}), \quad \forall j \in \mathbb{D} \quad (26)$$

These conditions are independent and specific to each space-

craft in a formation. Tolerance values δ^c and δ^d can be selected to trade off the energy costs associated with measurements and communication events against state estimation accuracy.

In fig. 3, the different stages of the event-trigger filtering for a formation flying are illustrated, where the independent sensor activations are displayed, including the stage where if no sensing is performed, the graph turns into communication nodes, with no measurements being exchanged between spacecraft, only non-sensing communications are being performed. The event-triggered conditions for both measurement sets is based exclusively on achieving adequate uncertainty levels for each individual filter and can be triggered independently. This improves upon existing consensus-based distributed event-triggered architectures that attempt to decrease the number of communication events by only transmitting local information when this is considered significant [30]. This constitutes a significant accuracy disadvantage since it relies on the ability to differentiate between relevant and irrelevant information, while our procedure is based on a lower bound on estimator uncertainty.

The main advantages of our Consider Covariance (CC) approach include:

- The ability to decouple the full formation filter into two smaller filter architectures corresponding to chief and deputies, with independent measurement models
- The ability to perform measurement updates independently on the chief and deputies using different event-triggering schemes, as discussed in the next section

6. PROPOSED LOW-COMMUNICATION DISTRIBUTED STATE-ESTIMATION FRAMEWORK

Taking into account the initially developed distributed state-estimation framework that guarantees deputy-chief correlations via *consider covariance* with the proposed event-trigger procedures, it is possible to formulate the filter algorithm that is summarized in algorithms 3 and 4.

The event-trigger procedures dictate when the update stage of the EKF occurs, deciding when to activate the sensors to improve the filter estimate. Otherwise, the filter only propagates the state by applying the spacecraft dynamic model equations, i.e $P_{k+1}^j = P_{k+1|k}^j$ and $\hat{x}_{k+1}^j = \hat{x}_{k+1|k}^j$. This corresponds to a sensor selection process that defines the instants when to perform each measurement set. The decoupled event-trigger scheme allows to optimize differently each measurement set, GPS and relative-range measurements, by not performing the update stage when the conditions are not met. Furthermore, these conditions are based on a mathematical estimation lower bound, the *Crámer-Rao Lower Bound* (CRLB), therefore the conditions maintain their consistency through any formation setting, without the need to manually adjust any threshold. These include a set of tolerance values that are adjusted based on the energy requirements of the mission and are not affected by the formation architecture.

The proposed model leads to a drastic reduction in terms of communications, as the chief and deputy have separate filter architectures that only transmit either individual measurements between deputies or the chief estimate and covariance matrix for the *consider covariance* strategy. In addition, with

Algorithm 3: Proposed Low-Communication Distributed State-Estimation Framework - Chief Filter Architecture

```

for  $i \in \mathbb{C}$  do
    1. Prediction Step:
         $\hat{x}_{k+1|k}^i = f(x_k^i, w_k^i);$ 
         $P_{k+1|k}^i = F_k^i P_k^i (F_k^i)^T + Q_k^i;$ 
    2. Event-Trigger Condition:
        if  $\beta^c$  then
            3. Update Step:
                 $K_{k+1}^i = P_{k+1|k}^i (H_{k+1}^i)^T \cdot$ 
                 $[H_{k+1}^i P_{k+1|k}^i (H_{k+1}^i)^T + R_{k+1}^i]^{-1};$ 
                 $P_{k+1}^i = (I - K_{k+1}^i H_{k+1}^i) \cdot P_{k+1|k}^i;$ 
                 $\hat{x}_{k+1}^i = \hat{x}_{k+1|k}^i + K_{k+1}^i \cdot [z^i - h(\hat{x}_{k+1|k}^i, v_{k+1}^i)];$ 
        4. Crámer-Rao Lower Bound:
         $J_{k+1}^i = ((F_k^i)^{-1})^T J_k^i ((F_k^i)^{-1}) + (H_{k+1}^i)^T (R_{k+1}^i)^{-1} H_{k+1}^i;$ 
         $(P_{k+1}^*)^{(i)} = (J_{k+1}^i)^{-1}$ 

```

the event-trigger conditions, the communications are reduced even further, by selecting the best instants to activate the sensors. The main advantages of this approach include:

- The ability to decouple the full formation filter into two smaller filter architectures corresponding to chief and deputies, with independent measurement models;
- The ability to perform measurement updates independently on the chief and deputies using different event-triggering schemes. This opens the possibility for sensor selection procedures that decide the best instants to activate the spacecraft sensors;
- An event-triggered framework that is based on the sequential CRLB and independent from the formation architecture or problem setting. It includes tolerance levels that balance between estimation accuracy and communication efficiency.

7. SIMULATION EXPERIMENTS

Mission Specifications

Our experiments target a four-satellite CubeSat formation base on the recent NASA V-R3x mission [24]. The initial positions are approximately the same for all satellites, with a semi-major axis of 6903 km, inclination of 97°, and eccentricity of 0.0012, but with different relative linear and angular velocities that make the spacecraft diverge along the orbit to a maximum relative distance of approximately 10 km.

State-Estimation Parameters

In this implementation, the state uncertainty for the chief, w_{k_1} , was modeled as a zero-mean Gaussian with a standard deviation of 10 cm for position, r_{w_1} , and 1 cm/s for the velocity, v_{w_1} , as a result the state process noise matrix can be defined as $Q_1 = I_{6 \times 6} \cdot [I_{3 \times 1} \cdot r_{w_1}^2; I_{3 \times 1} \cdot v_{w_1}^2](km/s)^2$. In regards to the deputies, the state uncertainty for the filter was modeled higher, as a zero-mean Gaussian with a standard deviation of 1 m for the position, r_{w_j} , and 1 cm/s for the velocity, v_{w_j} . In this case, the state process noise matrix can be defined as $Q_j = I_{6 \times 6} \cdot [I_{3 \times 1} \cdot r_{w_j}^2; I_{3 \times 1} \cdot v_{w_j}^2](km/s)^2$, $\forall j =$

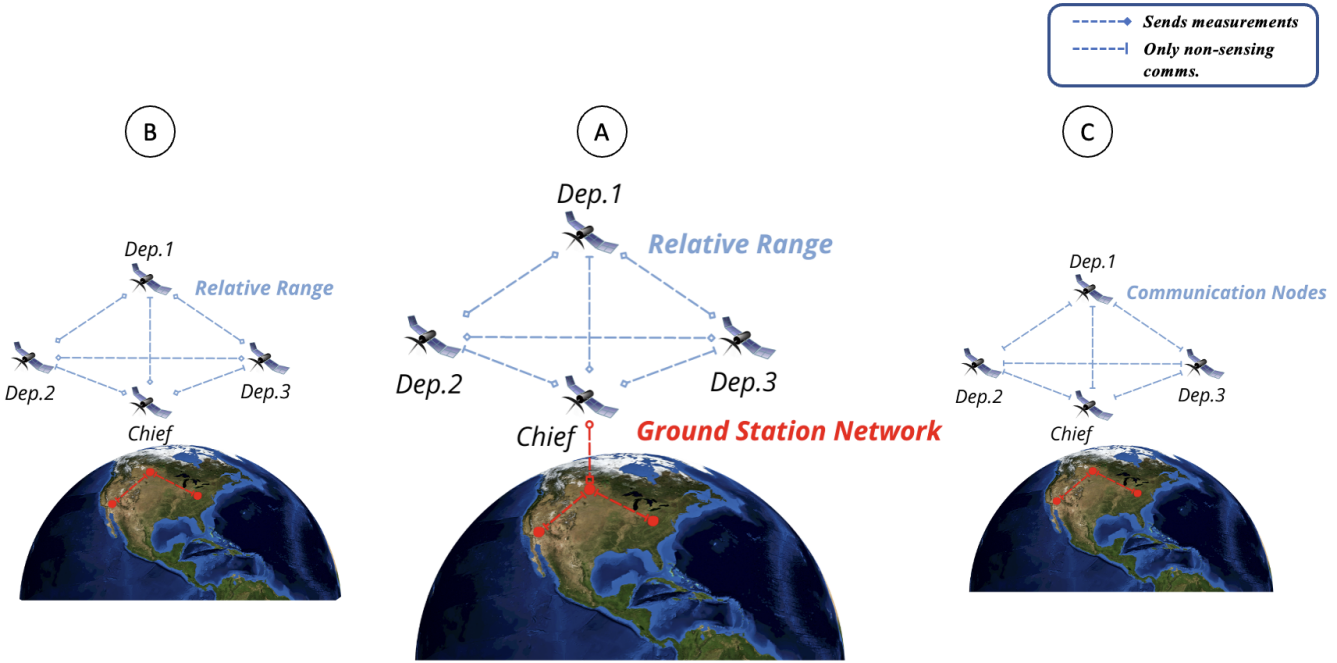


Figure 3. Satellite formation orbiting Earth in the different stages : (A) - Formation has both relative sensing (blue) between every satellite taken by each deputy and GPS measurements (red) from the chief; (B) - Only relative-range being used by deputies; (C) - No measurements are being actuated and the formation graph only contains communication nodes between spacecraft.

2, 3, 4. These values are based on uncertainty parameters obtained in the first *V-R3x* mission [24].

The measurement uncertainty corresponds to the values specific to the sensors in the *CubeSats*, more specifically each containing high-accuracy GPS units and also equipped with time-of-flight ranging. The measurement uncertainty for GPS measurements, $v_{k_{GPS}}$, is modeled by a zero-mean Gaussian with a standard deviation of 10 cm , while the uncertainty for the relative-range, $v_{k_{RR}}$, has a standard deviation of 1 m . In both cases, the measurement covariance matrix is given by $R = v_k \cdot I_{N \times N} (\text{km})^2$, where N corresponds to the number of measurements for the filter.

It is also important to note that throughout this section the consensus-based architecture corresponds to the consensus on the measurements version proposed by Battistelli [17], with the use of *Metropolis Weights*, a commonly used procedure in these filters to optimize accuracy results for the formation. In addition, the simulations will be tested through Monte-Carlo runs, with 100 samples, in which the initial positions will be placed 100 m away from the real initial position in a random direction, different for each simulation run, in addition to an added random velocity deviation equivalent to the state uncertainty for this component.

Accuracy Analysis

In this case, the *V-R3x* mission settings were used[24], in order to replicate the future mission environment that the code will be tested, the position error through time can be seen in fig. 4, where the confidence levels for both were set to $\delta^c = 5$ and $\delta^d = 1.5$. The Root Mean Squared Error (RMSE) results for the final orbit convergence error can be seen in

table 1, where the initial position errors are excluded as they correspond to an initial non-observable scenario where the relative distance between the spacecraft is very close, as a result, the relative sensing measurements between deputies have bad or no-information for the system correction.

The position error, in this case, is directly affected by the initial poorly observable scenario regarding the relative-range sensing, however taking into account the converged position error for the final simulation orbit, it is possible to see that the event-trigger variant has on-par RMSE with all the filters tested.

The table 1 shows that the fully distributed consensus-based and the distributed low-communication filter, with the *consider covariance* strategy, had on-par accuracy final converged error, 11.7 m and 11.5 m respectively, the latter with the closest performance to the best filter, the fully centralized unit with an averaged RMSE of 10.6 m . The worst results for the non event-trigger filters came from the naive version, that corresponds to the decoupled chief/deputy framework without the *consider covariance* implementation, it ended up reaching an error of 11.8 m .

In the end, both the consensus-based and the proposed framework with the *consider covariance* strategy provided close results to the fully centralized system, proving that the low-communication algorithm can be a viable option in this situation for a distributed framework. In addition, the event-triggered low-communication filter had an averaged RMSE of 12.6 m , that showcases what can be seen in fig. 4, that an already low-communication filter can be further optimized while maintaining the same accuracy levels.

Algorithm 4: Proposed Low-Communication Distributed State-Estimation Framework - Deputy Filter Architecture

for $j \in \mathbb{D}$ do

1. **Prediction Step:**

$$\begin{aligned}\hat{x}_{k+1|k}^j &= f(x_k^j, w_k^j); \\ P_{k+1|k}^j &= F_k^j P_k^j (F_k^j)^T + Q_k^j; \\ P_x^j &= F_k^j P_{xc}^j;\end{aligned}$$

2. **Event-Trigger Condition:**

if β^d then

3. **Relative-Range Measurements Exchange w/ Deputies:**

if $l \in \mathbb{D}$ then
 $z_j \leftarrow (z_l)$, where z_l corresponds to the local measurements of satellite l ;

4. **Consider Parameters - Communicate w/ Chiefs:**

for $i \in \mathbb{C}$ do

Communicate w/ each Chief Filter i from algorithm 3, to get consider variables $\mathbf{x}_{\text{Chief}}(i)$ and $P_{\text{Chief}}(i)$;

5. **Update Step:**

$$\begin{aligned}K_{k+1}^j &\leftarrow \text{Output from eq. (22)}; \\ \hat{x}_{k+1}^j &= \\ \hat{x}_{k+1|k}^j &+ K_{k+1}^j \cdot [z - h(\hat{x}_{k+1|k}^j, v_{k+1}^j, \mathbf{x}_{\text{Chief}})]; \\ P_{k+1}^j &\leftarrow \text{Output from eq. (24)}; \\ P_{xc}^j &= P_{xc}^j - K_k^j H_k^j P_{xc}^j - K_{k+1}^j H_c^j P_{\text{Chief}};\end{aligned}$$

6. **Crámer-Rao Lower Bound:**

$$\begin{aligned}J_{k+1}^j &= ((F_k^j)^{-1})^T J_k^j ((F_k^j)^{-1}) + (H_{k+1}^j)^T (R_{k+1}^j)^{-1} H_{k+1}^j; \\ (P_{k+1}^*)^{(j)} &= (J_{k+1}^j)^{-1}\end{aligned}$$

In the case of the distributed filters, both the consensus-based and the decoupled filters had a better convergence speed that can be explained by the effects of poorly observable measurements not affecting directly the information for the GPS measurements to the system. However, through time, once the relative-range measurements start providing more information to the system, the fully centralized unit converges to better position error results than the distributed filters, as it combines all the cross-correlations from the spacecraft measurement models in the same system.

Communication Network Optimization

The initially proposed decoupled event-triggered consider EKF has considerable benefits in optimizing the communication network of a small-satellite formation. As the event triggered condition tackles the sensor selection schedule, by defining the instants that each measurement set, either the GPS or relative-range, are activated, the first part of the analysis includes the proportion, with respect to the non-event-triggered proposed distributed framework, that the inclusion of the event triggered conditions saves in sensor activations. The fig. 5, illustrates, that by applying the proposed event-triggered conditions it is possible to have on-par accuracy levels while reducing the GPS measurements by $\approx 50\%$ and the range measurements by $\approx 43\%$. This corresponds exactly

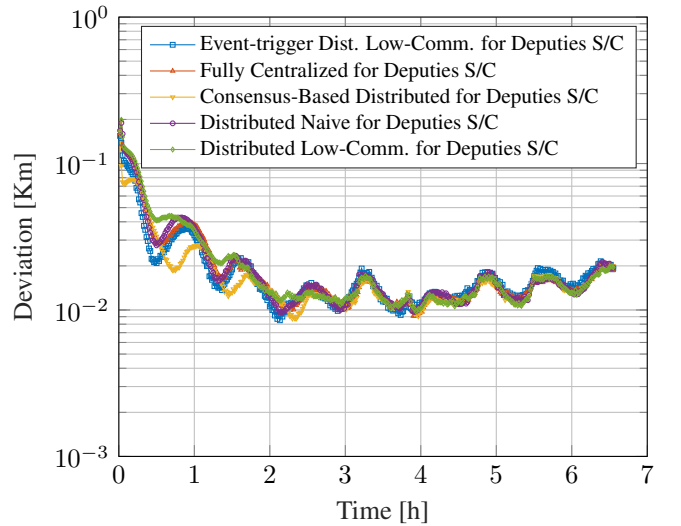


Figure 4. Monte-Carlo simulation for averaged absolute position error through time of different filters for the deputies with standard uncertainty conditions for the V-R3x mission setting.

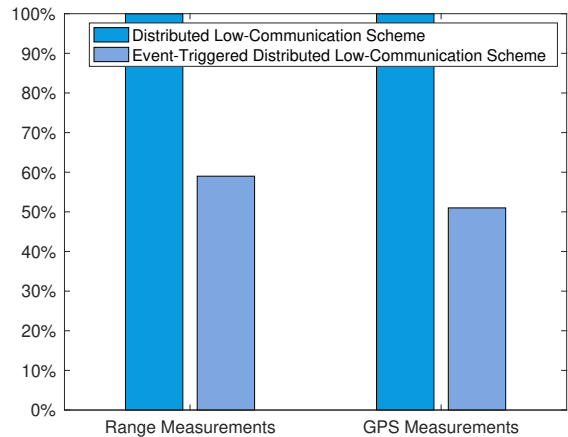


Figure 5. Bar chart illustrating the sensor activation proportion when comparing the event-triggered consider framework with the fully centralized filter as the baseline for the V-R3x mission setting.

to an optimized system for the V-R3x mission requirements that could only be reached by having a set of event triggered conditions that can be optimized by modifying the confidence level applied to each filter to have the same accuracy levels while relying more on relative-range measurements and minimizing drastically the expensive GPS measurements.

One of the most important points to make from these results is that the benefits of using the proposed event-triggered conditions depend on the specifications for each mission, in this case, an emphasis was made on maintaining the accuracy levels and diminishing the use of expensive GPS measurements, by relying more on the relative-range measurements. This was achieved by modifying accordingly the

Table 1. Simulation Results for the *V-R3x* Mission

Filter	Abs. Error S/C 1 [m]	Abs. Error S/C 2 [m]	Abs. Error S/C 3 [m]	Abs. Error S/C 4 [m]
Fully Centralized	0.157	11.4	12.2	18.5
Consensus-Based Distributed Scheme	0.168	13.4	15.1	18.1
Naive Distributed Scheme	0.168	13.1	14.6	19.3
Proposed Dist. Low-Comm. Framework	0.168	13.1	14.3	18.5
Event-Triggered Dist. Low-Comm. Framework	0.327	15.1	16.1	18.8

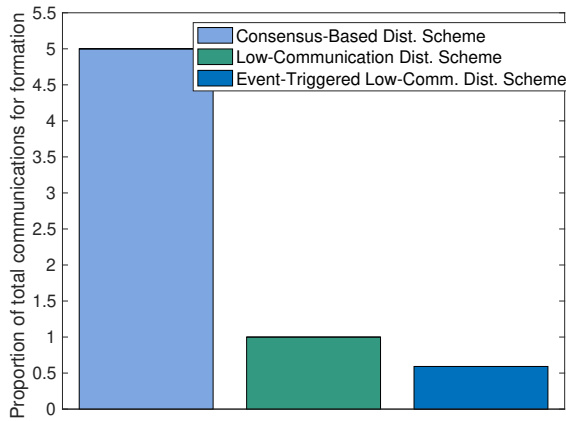


Figure 6. Analysis of the communication burdens between the distributed consensus-based scheme and the event-triggered consider a version with the proposed low-communications framework as baseline.

confidence levels that multiply with the filter lower-bound, if we increased them for a specific filter, it would mean that we have higher confidence in the sensing set, and desire to minimize the usage of these measurements.

A decoupled architecture such as the proposed low-communication framework relies, in the case of the deputies, on exchanging the independent measurements between spacecraft to perform the correction step of the EKF, as each deputy measurement model includes all the independent relative-range measurements of the formation. As a consequence, minimizing the sensing schedule of the formation will also result in minimizing the total number of communications in the formation.

As it can be seen in fig. 6, the consensus-based distributed filter has 5 times more communications than our distributed low-comm. scheme. This is due to the number of iterations in the consensus rounds being $L = 5$ in the simulations performed, as this is considered to be the common value for the formation size [25]. The difference between the two methods comes from the proposed framework not using the consensus rounds, which rely on constant communication and exchange of information between the different spacecraft through L consensus steps, in order to reach a consensus average for the formation. The proposed scheme does not need to continuously exchange measurements, as it maintains the distributed scheme by each spacecraft having its independent filter with a decoupled architecture from deputies and chief, while exchanging directly the measurements between spacecraft with the same measurement model, and using the *consider covariance* strategy to introduce the cross-correlations

from other satellites with a different measurement set.

In the case of the improvements when adding the event triggered conditions to the consider filter, the implementation of sensor selection procedures improves the total number of communications by 43% from the proposed low-communications network. This difference can be explained by the saved relative sensing activation's of $\approx 43\%$ seen in fig. 5, as the measurement model in the update stage of the EKF requires the communication with remaining spacecraft in the formation, in this case, three other satellites, where in the case of the deputies the measurements are exchanged and in the case of the chief, the covariance matrix and position estimate of its filter are exchanged.

It is also important to remark that the communication efficiency, i.e. the number of communications saved in comparison with the standard *consider covariance* filter could be further enhanced depending on the mission specifications, by increasing the confidence value regarding the relative-range measurements. However, this is not the intention of the mission, as we desire to maintain the same accuracy levels and focus on minimizing the expensive GPS measurements, which as a result does not allow us to minimize even more the communications in the network, since the update step of the chief filter does not require extra communications while in the case of the deputies, that use relative-range, to perform the update stage the communications between all the satellites is required.

In regards to the final evaluation criteria for the communication network efficiency, the total memory transferred between all the satellites in the formation for the entire simulation can be seen in fig. 7. In this case, the results show that in the proposed low-communication framework with the implementation of the event triggered conditions over ≈ 4 orbits, the total memory transferred for the formation is 1000 times bigger if the formation uses a localization procedure based on consensus filtering than the proposed algorithm.

The memory calculations for a given time instant are detailed for both the proposed event-triggering distributed low-communication framework and the distributed consensus-based framework in table 2. In this representation, it is possible to understand the memory requirements for each framework by comparing the transferred variable in each filter for a given time instant, and the final calculations correspond to the total memory requirements for the formation flying. The consensus-based procedures continuously exchange matrices $(\delta\Omega^{(i)}, \delta q^{(i)})$, that correspond to the (unique) elements of the (symmetric) novel information matrix and vector, where the state includes all the spacecraft in the formation, in this case for a four satellite formation, corresponds to 24 equations, over multiple consensus rounds. However, the proposed architecture only exchanges between spacecraft a small covariance matrix and a chief state with 6 dynamics equations and individual values corresponding to the independent measurements.

Table 2. Memory Analysis per iteration for a four spacecraft formation with Chief/Deputy setting.

Filter	Framework	Transferred Variable	Memory Requirements
Chief Filter	Proposed Low-Communications	$x_{chief}; P_{chief}$	$\sum_{i=1}^D 8 \cdot 6 + 8 \cdot (6 \cdot 6) = 1008 \text{ bytes}$
Chief Filter	Consensus-Based	$\delta\Omega^{(i)}; \delta q^{(i)}$	$\sum_{l=1}^L 8 \cdot (24 \cdot 24) + 8 \cdot (24 \cdot 1) = 19.2 \text{ Kbytes}$
Deputy Filter	Proposed Low-Communications	$y_{pq}^{(i)}$, where $p \neq j, \forall \{p, q\} \neq i$	$\sum_{i=1}^D 8 \cdot 3 = 72 \text{ bytes}$
Deputy Filter	Consensus-Based	$\delta\Omega^{(j)}; \delta q^{(j)}$	$\sum_{l=1}^L 8 \cdot (24 \cdot 24) + 8 \cdot (24 \cdot 1) = 19.2 \text{ Kbytes}$

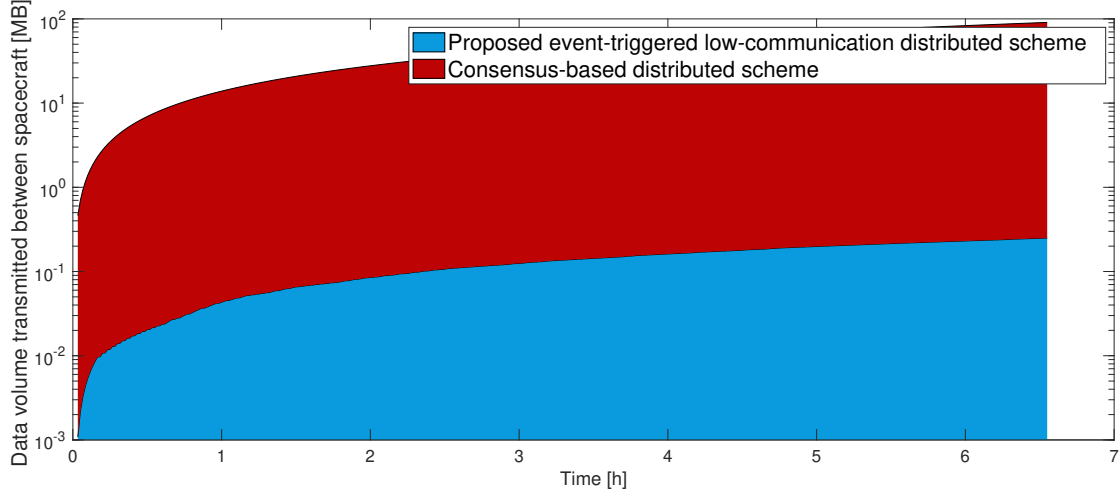


Figure 7. Data volume transmitted between spacecraft in the formation for the proposed framework (blue) and the distributed consensus-based filter of Battistelli [17] (red).

8. CONCLUSIONS

This paper presented a novel distributed low-communications framework that is able to provide the following benefits compared to previous consensus-based filtering algorithms:

- An event-triggered procedure for sensor selection in which the trigger conditions include user-defined confidence levels specific for each sensor type that are proportional to the CRLB and allow the designer to explicitly trade-off accuracy and communication;
- Similar accuracy with a 43% reduction in communication events in the *V-R3x* mission scenario;
- Reduction in data volume transferred between spacecraft by a factor of 1000;

The proposed distributed low-communication framework shows great potential as a viable and innovative solution for on-board satellite formation localization systems that follow the chief/deputy formation architecture. In future work, we will pursue:

- The minimization of relative orbit ambiguities in measurement models that have relative-range sensing[31]. This could be reached through increasing the dynamic model for higher-order terms or in the control segment through selective control inputs based on their information matrix;
- The development of an extension of the event-triggered conditions that can take full advantage of the *consider covariance* strategy as a tool to measure the impact of neglecting the external input uncertainties in the model, in this case, the chief estimate uncertainty, when compared to the naive covariance matrix;
- The study of the optimization of the tolerance levels that

d dictate the proportion of sensor activations. The tolerance, depends not only on the mission specifications, if there are heavy communications constraints or if there are only computing power limits, but they also depend on the information levels the sensors can reach. For example, to minimize the GPS communications to 50% you only need a small tolerance, as these are very strong measurements, whereas relative-range in a very ambiguous environment, this term needs to be much higher to reach the same amount of sensor activation gains;

ACKNOWLEDGMENTS

The authors would like to thank the *Fulbright Portugal Commission* and *Fundaçao Luso-Americana Para O Desenvolvimento* for the continuous support throughout the duration of the research. This work was partially supported by the LARSyS - FCT Project UIDB/50009/2020.

REFERENCES

- [1] M. Veloso, J. Biswas, B. Coltin, S. Rosenthal, T. Kollar, C. Mericli, M. Samadi, S. Brandão, and R. Ventura, “Cobots: Collaborative robots servicing multi-floor buildings,” in *2012 IEEE/RSJ International Conference on Intelligent Robots and Systems*, 2012, pp. 5446–5447.
- [2] M. Bualat, J. Barlow, T. Fong, C. Provencher, and T. Smith, “Astrobee: Developing a free-flying robot for the international space station,” in *AIAA SPACE 2015 Conference and Exposition*, August 2015.

- [3] C. T. Fraser, “Adaptive Extended Kalman Filtering Strategies for Autonomous Relative Navigation of Formation Flying Spacecraft,” Master’s thesis, Carleton University, 2019.
- [4] P. R. Cachim, J. Gomes, and R. Ventura, “Autonomous orbit determination for satellite formations using relative sensing: Observability analysis and optimization,” *Acta Astronautica*, vol. 200, pp. 301–315, November 2022. [Online]. Available: <http://arxiv.org/abs/2109.09186>
- [5] Z. Manchester, M. Peck, and A. Filo, “KickSat: A crowd-funded mission to demonstrate the world’s smallest spacecraft,” in *AIAA/USU Conference on Small Satellites (SmallSat)*, Logan, UT, August 2013. [Online]. Available: https://rexlab.stanford.edu/papers/KickSat_SmallSat.pdf
- [6] M. Holliday, A. Ramírez, C. Settle, T. Tatum, D. G. Senesky, and Z. Manchester, “Pycubed: An open-source, radiation-tested cubesat platform programmable entirely in python,” *AIAA/USU Conference on Small Satellites (SmallSat)*, 2019.
- [7] *Mars Architecture Strategy Working Group (MASWG)*, Jakosky, and B. M. et al, “Mars, the nearest habitable world — A comprehensive program for future Mars exploration,” *NASA Mars Architecture Strategy Working Group*, 2020.
- [8] European Comission. (2020, February) Advancing the feasibility of self-organising small satellite formations. <https://cordis.europa.eu/article/id/413502-advancing-the-feasibility-of-self-organising-small-satellite-formations>.
- [9] H. E. Spence, “Helioswarm: Unlocking the multiscale mysteries of weakly-collisional magnetized plasma turbulence and ion heating,” *American Geophysical Union, Fall Meeting*, December 2019.
- [10] S. Bandyopadhyay, R. Foust, G. P. Subramanian, S.-J. Chung, and F. Y. Hadaegh, “Review of formation flying and constellation missions using nanosatellites,” *Journal of Spacecraft and Rockets*, vol. 53, no. 3, pp. 567–578, 2016.
- [11] A. Caspi, M. Barthelemy, C. D. Bussy-Virat, I. J. Cohen, C. E. DeForest, D. R. Jackson, A. Vourlidas, and T. Nieves-Chinchilla, “Small satellite mission concepts for space weather research and as pathfinders for operations,” *Space Weather*, vol. 20, no. 2, January 2022.
- [12] R. Staehle, D. Blaney, H. Hemmati, D. Jones, A. Klesh, P. Liewer, J. Lazio, M. Lo, P. Mouroulis, N. Murphy, P. Pieingree, T. Wilson, P. Puig-suari, A. Williams, T. Svitek, B. Betts, and L. Friedman, “Interplanetary Cubesat architecture and missions,” *AIAA SPACE Conference and Exposition 2012*, Setembre 2012.
- [13] J. Wang and E. Butcher, “Decentralized estimation of spacecraft relative motion using consensus extended kalman filter,” in *2018 Space Flight Mechanics Meeting*, January 2018.
- [14] R. Olfati-Saber, “Kalman-consensus filter : Optimality, stability, and performance,” in *Proceedings of the 48h IEEE Conference on Decision and Control (CDC) held jointly with 2009 28th Chinese Control Conference*, 2009, pp. 7036–7042.
- [15] D. Dumitriu, S. Marques, P. U. Lima, and B. Udrea, “Decentralized, low-communication state estimation and optimal guidance of formation flying spacecraft,” in *AAS 06-158*, 2006.
- [16] G. Battistelli and L. Chisci, “Kullback–Leibler average, consensus on probability densities, and distributed state estimation with guaranteed stability,” *Automatica*, vol. 50, no. 3, pp. 707–718, 2014.
- [17] ———, “Stability of consensus extended Kalman filter for distributed state estimation,” *Automatica*, vol. 68, pp. 169–178, 2016.
- [18] J. H. Taylor, “The Cramer-Rao estimation error lower bound computation for deterministic nonlinear systems,” in *1978 IEEE Conference on Decision and Control including the 17th Symposium on Adaptive Processes*, 1978, pp. 1178–1181.
- [19] S. Liu, E. Masazade, M. Fardad, and P. K. Varshney, “Sensor selection with correlated measurements for target tracking in wireless sensor networks,” in *2015 IEEE International Conference on Acoustics, Speech and Signal Processing (ICASSP)*, 2015, pp. 4030–4034.
- [20] M. Ribeiro and I. Ribeiro, “Kalman and extended Kalman filters: Concept, derivation and properties,” *Institute for Systems and Robotics*, May 2004.
- [21] R. E. Kalman, “A New Approach to Linear Filtering and Prediction Problems,” *Journal of Basic Engineering*, vol. 82, no. 1, pp. 35–45, 03 1960.
- [22] M. E. Lisano, “Comparing consider-covariance analysis with sigma-point consider filter and linear-theory consider filter formulations,” in *Proceedings if 20th International Symposium on Space Flight Dynamics, Annapolis*, 2007.
- [23] O. Montenbruck and E. Gill, *Satellite Orbits*. Springer, January 2000, vol. 1.
- [24] M. Holliday, K. Tracy, Z. Manchester, and A. Nguyen, “The V-R3X mission: Towards autonomous networking and navigation for Cubesat swarms,” *The 4S Symposium 2022*, 2022.
- [25] G. Battistelli, L. Chisci, G. Mugnai, A. Farina, and A. Graziano, “Consensus-based linear and nonlinear filtering,” *IEEE Transactions on Automatic Control*, vol. 60, no. 5, pp. 1410–1415, 2015.
- [26] K. Matsuka, A. O. Feldman, E. S. Lupu, S.-J. Chung, and F. Y. Hadaegh, “Decentralized formation pose estimation for spacecraft swarms,” *Advances in Space Research*, vol. 67, no. 11, pp. 3527–3545, 2021.
- [27] J. Hinks and M. Psiaki, “A multipurpose consider covariance analysis for square-root information filters,” in *AIAA Guidance, Navigation, and Control Conference 2012*, August 2012.
- [28] A. Nordio, A. Tarable, F. Dabbene, and R. Tempo, “Sensor selection and precoding strategies for wireless sensor networks,” *IEEE Transactions on Signal Processing*, vol. 63, no. 16, pp. 4411–4421, 2015.
- [29] S. Joshi and S. Boyd, “Sensor selection via convex optimization,” *IEEE Transactions on Signal Processing*, vol. 57, no. 2, pp. 451–462, 2009.
- [30] G. Battistelli, L. Chisci, and D. Selvi, “A distributed kalman filter with event-triggered communication and guaranteed stability,” *Autom.*, vol. 93, pp. 75–82, 2018.
- [31] J. Wang, E. Butcher, and T. Lovell, “Ambiguous relative orbits in sequential relative orbit estimation with range-only measurements,” *Acta Astronautica*, vol. 151, July 2018.

BIOGRAPHY



Rafael Cordeiro is an international visiting student with the Robotic Exploration Lab at Carnegie Mellon University (CMU), with a BS degree from Instituto Superior Técnico (IST) in 2020. He is a recipient of a scholarship from Fulbright for research on optimized distributed localization systems for Cubesats. He is also a recipient of a scholarship from the Massachusetts Institute of Technology (MIT) Portugal program for 2022. His research interests include optimization procedures for spacecraft navigation and guidance systems.



João Gomes is an Associate Professor at Instituto Superior Técnico (IST), Universidade de Lisboa, Portugal, and a senior researcher in the Signal and Image Processing Group of the Institute for Systems and Robotics. He received the Diploma, M.S., and Ph.D. degrees in electrical and computer engineering from IST in 1993, 1996, and 2002, respectively. His research interests include estimation and localization/tracking in aerospace and GPS-denied environments, signal processing for telecommunications in harsh environments, and distributed signal processing algorithms. He currently serves as an Associate Editor for signal processing and communications in the IEEE Journal of Oceanic Engineering.



Rodrigo Ventura (PhD) is a tenured Assistant Professor of the Electrical and Computer Engineering Department of Instituto Superior Técnico (IST), University of Lisbon, and a senior researcher of the Institute for Systems and Robotics (ISR-Lisbon). He has published more than 130 publications in peer-reviewed international journals and conferences, and is also co-inventor of several national and international patents on innovative solutions for robotic systems. Broadly, his research is focused on the intersection between Robotics and Artificial Intelligence. This research is driven by applications in space robotics, urban search and rescue robotics, aerial robots, and social service robots.



Zachary Manchester is an assistant professor in the Robotics Institute at Carnegie Mellon University and founder of the Robotic Exploration Lab. He received a PhD in aerospace engineering in 2015 and a BS in applied physics in 2009, both from Cornell University. His research interests include control and optimization with application to aerospace and robotic systems with challenging nonlinear dynamics.